ADVANCED ENERGY MATERIALS
www.advenergymat.de

Materials Views
www.MaterialsViews.com

Electrochemical Performance of Porous Carbon/Tin Composite Anodes for Sodium-Ion and Lithium-Ion Batteries

*Yunhua Xu, Yujie Zhu, Yihang Liu, and Chunsheng Wang**

The electrochemical performance of mesoporous carbon (C)/tin (Sn) anodes in Na-ion and Li-ion batteries is systematically investigated. The mesoporous C/Sn anodes in a Na-ion battery shows similar cycling stability but lower capacity and poorer rate capability than that in a Li-ion battery. The desodiation potentials of Sn anodes are approximately 0.21 V lower than delithiation potentials. The low capacity and poor rate capability of C/Sn anode in Na-ion batteries is mainly due to the large Na-ion size, resulting in slow Na-ion diffusion and large volume change of porous C/Sn composite anode during alloy/dealloy reactions. Understanding of the reaction mechanism between Sn and Na ions will provide insight towards exploring and designing new alloy-based anode materials for Na-ion batteries.

1. Introduction

Li-ion batteries have been widely employed in portable electronic devices and are expected to power electric vehicles and even to be used as energy storage components in grid harvesting from renewable energy sources. Taking into account that the lithium resource is limited and unevenly distributed around the world, for future large-scale commercial manufacture of Li-ion batteries cost would become a major issue. Sodium, in contrast, is abundant and available around the world. Na-ion batteries are attractive for applications in smart electric grids that integrate discontinuous energy flow from renewable sources optimizing the performance of clean energy sources. Actually, sodium has been successfully used in commercial Na–S rechargeable batteries, which operate at a temperature of 300 °C or higher in a molten state.[1]

Recently, room temperature sodium-ion (Na-ion) batteries have received growing interest spurred by the rapid advance in rechargeable battery technology and fast increasing demand in the market.[2–15] However, Na ions are about 55% larger in radius than Li ions, which makes it more difficult for them to be reversibly inserted into and extracted from host materials.[2] Among numerous electrode materials for Li-ion batteries,[16–23] only a few are suitable host materials to accommodate Na ions and allow reversible insertion/deinsertion reactions; most of these are cathode materials.[8–15] So far, very few anode materials have been reported for Na-ion batteries. Porous carbon has been identified as one such anode material.[3,4] In porous carbon, Na ions can be reversibly inserted into nanopores or absorbed on the surface of carbon, providing capacity of less than 200 mA h g^{-1}. Recently, Xiao et al. reported that SnSb/C nanocomposite, an anode material for Li-ion batteries, can also reversibly alloy with Na providing good cycling stability and rate capability.[2] On the basis of theoretical calculation, Ceder and colleagues predicted that Sn can electrochemically react with sodium to yield the final alloy formula of $Na_{15}Sn_4$, corresponding to a theoretical capacity of 851 mA h g^{-1}.[6] These studies clearly demonstrated that Sn is an attractive anode material for Na-ion batteries.

In this paper, the electrochemical performance of a mesoporous C/Sn composite anode in Na-ion batteries is investigated and compared with the behavior in Li-ion batteries. The purpose of using mesoporous C/Sn composites rather than Sn nanoparticles is to effectively stabilize Sn nanoparticles via the mesoporous carbon matrix during ion insertion/extraction,[23] especially for Na ions with larger ion size than Li ions.

2. Results and Discussion

A porous C/Sn composite with Sn content of 66 wt% was synthesized by dispersing SnO_2 nanoparticles into a soft-template polymer matrix followed by carbonization.[23] Detail synthesis procedure can be found in the Supporting Information. Briefly, SnO_2 nanoparticles were first dispersed into the nanophase-patterned polymer matrix, where resorcinol–formaldehyde (RF) resin was used as carbon source and a block copolymer, poly(ethylene oxide)-*block*-poly(propylene oxide)-*block*-poly(ethylene oxide) (EO_{106}-PO_{70}-EO_{106}; Pluronic F127), was introduced as a sacrificed soft template to create nanopores. The phase separation between these two polymers promoted a self-assembled nanostructure. During the following carbonization process, the template copolymer decomposed to

Dr. Y. Xu, Y. Zhu, Y. Liu, Prof. C. Wang
Department of Chemical and Biomolecular Engineering
University of Maryland
College Park, MD 20742, USA
E-mail: cswang@umd.edu

DOI: 10.1002/aenm.201200346

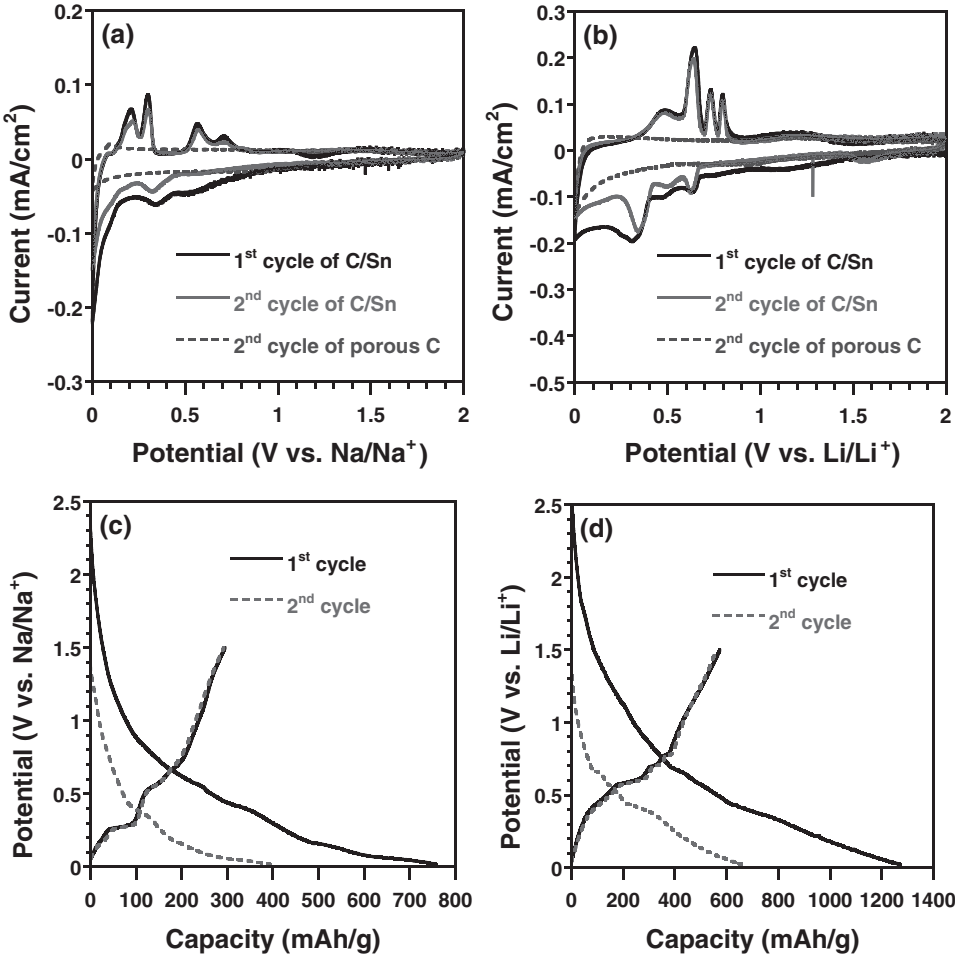

Figure 1. Cyclic voltammograms of mesoporous C/Sn anodes in a) Sn–Na and b) Sn–Li batteries at a scan rate of 0.05 mV s^{-1} between 0 and 2 V, and potential profiles of the mesoporous C/Sn anodes in c) Sn–Na and d) Sn–Li batteries during the first two galvanostatic charge/discharge cycles between 0.02 and 1.5 V at a current density of 20 mA g^{-1}.

form pores, the RF resin was carbonized to carbon frames, and SnO_2 nanoparticles were reduced to Sn nanoparticles by carbon at high temperature.

The Sn nanoparticles with a diameter of about 100 nm are uniformly dispersed in a porous carbon matrix, as demonstrated in scanning electron microscopy (SEM) images (Figure S1 in the Supporting Information). Pores with a size of approximately 10 nm are separated by ultrathin carbon walls. High-resolution transmission electron microscopy (HRTEM) and X-ray diffraction (XRD) measurements indicate that the nanoparticles in the carbon matrix are crystalline tin metal;[23] no SnO_2 was detected, indicating that the SnO_2 particles were completely converted to crystal tin. For comparison, porous carbon without Sn was also synthesized using the same procedure.

The electrochemical performance of the mesoporous C/Sn composite anodes for Na-ion and Li-ion batteries was investigated using coin cells. For Na-ion batteries, sodium and 1 M $NaClO_4$ in a mixture of ethylene carbonate/dimethyl carbonate (EC/DMC, 1:1 by volume) were used as the counter electrode and the electrolyte, respectively; while for Li-ion batteries, lithium was used as a counter electrode and 1 M $LiPF_6$ in a mixture of ethylene carbonate/diethyl carbonate (EC/DEC, 1:1 by volume) was used as electrolyte.

Figure 1a and b show the cyclic voltammograms (CV) of a mesoporous C/Sn anode in the first two cycles and a mesoporous C control anode in the second cycle at a scan rate of 0.05 mV s^{-1} between 0.0 and 2.0 V in Na-ion and Li-ion cells, respectively. The mesoporous carbon anodes in both Na-ion and Li-ion cells show a smooth current response during potential scan, and no obvious current peak can be observed, which are typical cycling voltammetry curves of carbon for Na-ion and Li-ion insertion/extraction.[2,4] Therefore, the well-defined current peaks in Figure 1a and b are attributed to ion insertion/extraction in Sn for both Sn–Na and Sn–Li batteries. In an anodic scan of porous Sn/C composite for Sn–Na batteries, four anodic peaks at 0.2, 0.3, 0.56, and 0.7 V, which are absent in mesoporous carbon, are attributed to the desodiation of $Na_{15}Sn_4$, Na_9Sn_4, NaSn, and $NaSn_5$, respectively (Figure 1a). These desodiation potentials are in good agreement with the calculated four potential plateaus at 0.11, 0.16, 0.47, and 0.68 V,

respectively, by Ceder's group if approximately 0.1 V overpotential is considered due to the slow Na diffusion in Sn during the CV scan.[5] The first cathodic scan shows a wide irreversible current peak in the range of 0.9 to 0.5 V, which corresponds to the decomposition of electrolyte to form solid–electrolyte interface (SEI) films.[2] Two reduction peaks at 0.5 V and 0.35 V and two barely visible shoulders at 0.15 and 0.1 V in sodiation scan can be assigned to the formation of corresponding four Na_xSn alloys.

Similar to the desodiation process, the delithiation of mesoporous C/Sn anodes at the same scan rate also presents four distinct oxidation peaks but at higher potentials (0.43, 0.65, 0.73, and 0.8 V; Figure 1b). The desodiation potentials of Sn anodes are approximately 0.21 V lower than delithiation potentials, which is close to the calculated value of approximately 0.15 V predicted by Ceder's group.[6] The potential difference of 0.06 V between experimental date and the theoretically calculated value could be attributed to the overpotential caused by the slow Na-ion diffusion in the anode electrode. The lithiation of Sn anodes presents three reversible peaks at 0.34, 0.5, and 0.62 V, which are associated with the lithiation reactions between Sn and Li (Figure 1b). A broad peak centered at 1.2 V (starting at 1.5 V and ending at 0.7 V) can be observed in the first lithiation, but disappears in the second cycle. This peak may be attributed to the decomposition of electrolyte to form SEI films, resulting in irreversible capacity.[24] The CV curves in Figure 1a and b demonstrate that the potential for SEI formation on Sn anodes in Na-ion batteries is lower than that in Li-ion batteries.

The difference in electrochemical behavior of Sn anodes in Na-ion and Li-ion batteries can also be observed in the galvanostatic charge/discharge between 0.02 and 1.5 V at 20 mA g^{-1} (Figure 1c and d). The ion extraction voltages for both Na and Li ions show sequential stepwise potential plateaus, but the desodiation plateaus of Na_xSn are 0.15–0.2 V lower than the delithiation plateaus of Li_xSn. The charge (ion extraction) capacity of C/Sn anodes in Na-ion batteries is 295 mA h g^{-1}, which is also smaller than that (574 mA h g^{-1}) in Li-ion batteries. Since the capacity of porous carbon without Sn are around 170 mA h g^{-1} for desodiation and around 300 mA h g^{-1} for delithiation at the same current density of 20 mA g^{-1} (Figure S2 in the Supporting Information), the capacity delivered by tin will be 359 mA h g^{-1} for desodiation and 715 mA h g^{-1} for delithiation, corresponding to 42% and 72% of the theoretical values, respectively (851 mA h g^{-1} for sodium and 992 mA h g^{-1} for lithium). The lower capacity utilization of Sn anodes in Na-ion batteries than in Li-ion batteries is mainly due to poor electrochemical sodiation/desodiation kinetics because Na ions are about 55% larger than Li ions in radius.[2] The large irreversible capacities of porous C/Sn anodes for both Na-ion and Li-ion batteries observed in Figure 1c and d are mainly contributed from porous carbon (Figure S2 in the Supporting Information). It is noteworthy that the similar charge capacities in the first two cycles for both Na-ion and Li-ion batteries demonstrate good electrochemical reversibility of the porous C/Sn composite.

Figure 2 compares the cycling stability of mesoporous C/Sn anodes in Na-ion and Li-ion batteries. The mesoporous C/Sn composite shows similar capacity decay rate in both Na-ion and Li-ion batteries although their initial capacities are different. The change in structure and morphlogy of the C/Sn anodes

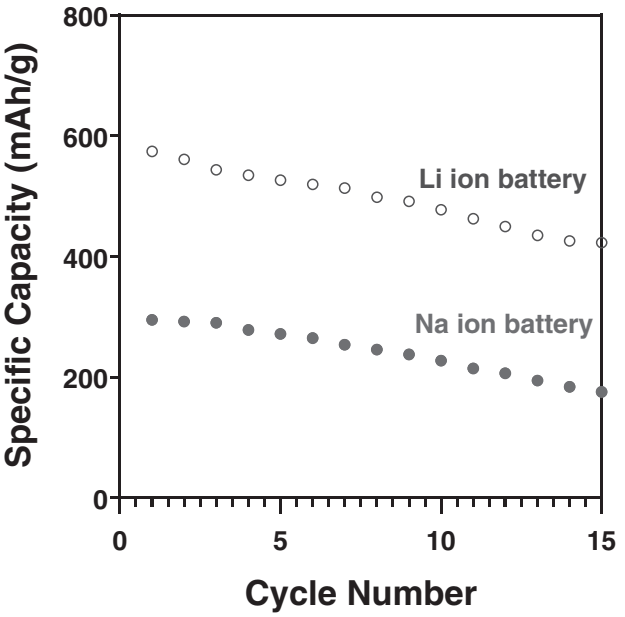

Figure 2. Capacity performance of mesoporous C/Sn anodes during charge/discharge cycles at 20 mA g^{-1} in Na-ion and Li-ion batteries.

during charge/discharge cycles in Li-ion and Na-ion cells were investigated using SEM and XRD. Figure S3 in the Supporting Information shows the XRD patterns of C/Sn anodes both fresh and after the 15th ion extraction. Crystal Sn peaks in Figure S3 can be clearly observed for the fresh and cycled C/Sn anodes, demonstrating that Sn in C/Sn anodes still retains its crystal structure after the 15th charge/discharge cycle in both Na-ion and Li-ion batteries. The Cu paterns in Figure S3 in the Supporting Information are attributed to the Cu current collector.

To understand the mechanism behind the lower capacity utilization of the mesoporous C/Sn composite in Na-ion batteries than in Li-ion batteries, the reaction resistances of mesoporous C/Sn anodes at different charge/discharge levels in Na-ion and Li-ion batteries were compared using a galvanostatic intermittent titration technique (GITT). During GITT measurements, the mesoporous C/Sn anodes were charged/discharged using a series of current (10 mA g^{-1} for Na-ion cells and 20 mA g^{-1} for Li-ion cells) pulses of equal duration (0.5 h). Following each pulse, the batteries were left on open circuit for 4 h to reach equilibrium potentials. **Figure 3**a and b show the potential response of mesoporous C/Sn anodes during GITT measurement in Na-ion and Li-ion batteries, respectively. The dotted-lines in Figure 3a and b represent equilibrium open-circuit voltages (OCVs). The overpotential for mesoporous C/Sn anodes in Na-ion batteries displays a gradual increase in charge reaction (ion extraction) and decrease in discharge reaction (ion insertion); in Li-ion batteries it is almost constant during discharge and charge processes except at the end of each process. The reaction resistances of mesopore C/Sn anodes in Na-ion and Li-ion batteries at different ion insertion levels were calculated by dividing the overpotential by the pulse current, as shown in Figure 3c and d. Similar to the overpotential shown in Figure 3a and b, the mesoporous C/Sn anodes show a relatively

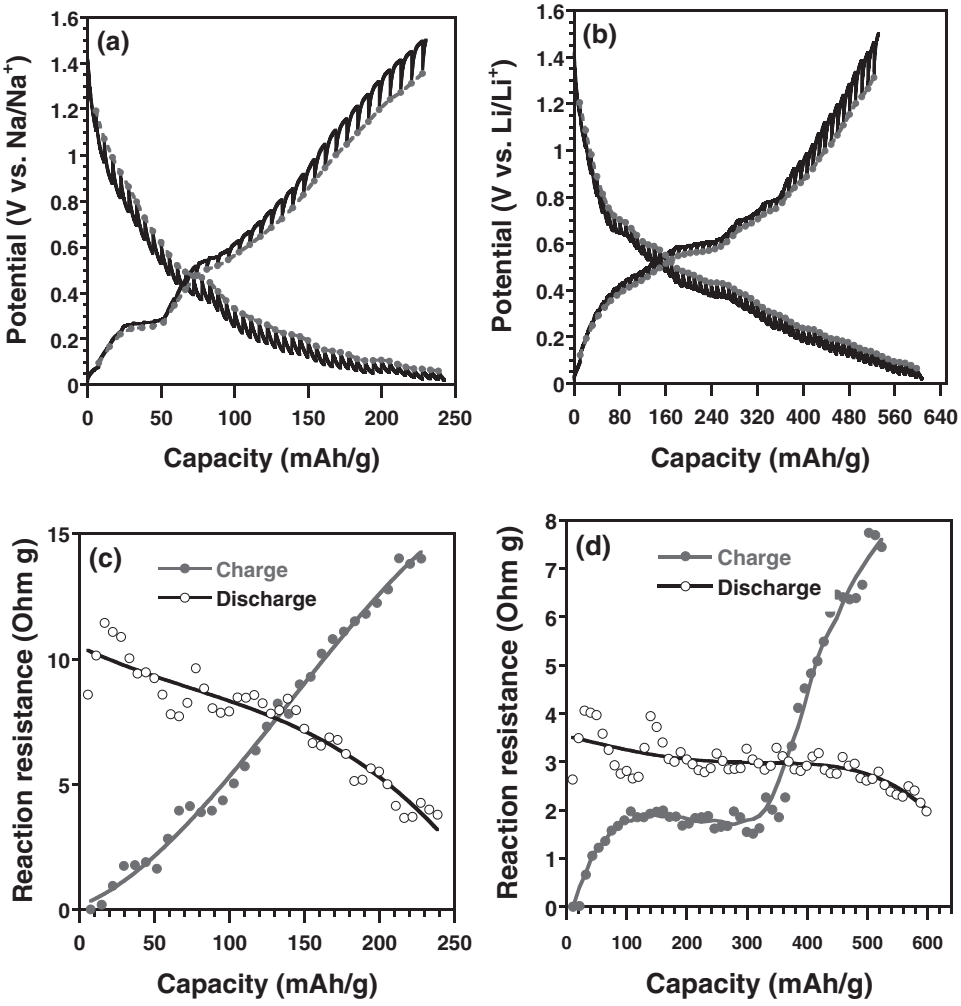

Figure 3. a,b) Potential response, and c,d) reaction resistance of mesoporous C/Sn anodes during GITT measurement (a,c) in an Na-ion cell at 10 mA g^{-1}, and (b,d) in an Li-ion cell at 20 mA g^{-1}.

stable reaction resistance during lithiation and delithiation except at the end of charge/discharge in Li-ion batteries. However, a slow decrease of reaction resistance during sodiation but quick increase of reaction resistance during desodiation were observed in Na-ion batteries. The average resistance of mesoporous C/Sn anodes in Na-ion batteries is at least two times higher than that in Li-ion batteries. The almost linear change of reaction resistance with Na content may be attributed to a large volume change of Na–Sn alloys. The volume increases during sodiation improve the contact between particles, reducing the reaction resistance. In contrast, the C/Sn composite particles will be separated from each other when particle size decreases during desodiation, resulting in a increase in resistance. At the end of charge, the reaction resistances reach the highest values in both Na-ion and Li-ion batteries.

The detailed reaction kinetics of the mesoporous C/Sn composite at the end of charge (largest reaction resistances) in Na-ion and Li-ion batteries were investigated using electrochemical impedance spectroscopy (EIS) in the frequency range 10 MHz to 0.01 Hz at 10 mV amplitude. **Figure 4** shows a representative Nyquist plot of mesoporous C/Sn anodes after being charged to 2 V at 20 mA g^{-1} in the 5th cycle with a subsequent relaxation period of 2 h. The impedance spectra are composed of one depressed semicircle at high frequencies and a straight slopping line at low frequencies. The depressed semicircle at high frequencies is associated with two overlapped interface impedances (i.e., SEI and charge-transfer impedance), and the low-frequency line corresponds to ion diffusion.[25] The much longer low-frequency sloping line of mesoporous C/Sn anodes in Na-ion cells than that in Li-ion cells confirms that transport of Na ions in Sn is much slower than that of Li ions. In addition to the high diffusion resistance, mesoporous C/Sn anodes also experienced a large interface impedance in Na-ion cells. The large interface impedance of mesoporous C/Sn anodes in Na-ion cells could be attributed to either high SEI film resistance or large charge-transfer resistance.

Due to the high reaction impedance and large overpotential of mesoporous C/Sn anodes in Na-ion batteries, the mesoporous C/Sn anodes also show poor rate capacity in Na-ion batteries. **Figure 5**a shows the rate performance of mesoporous

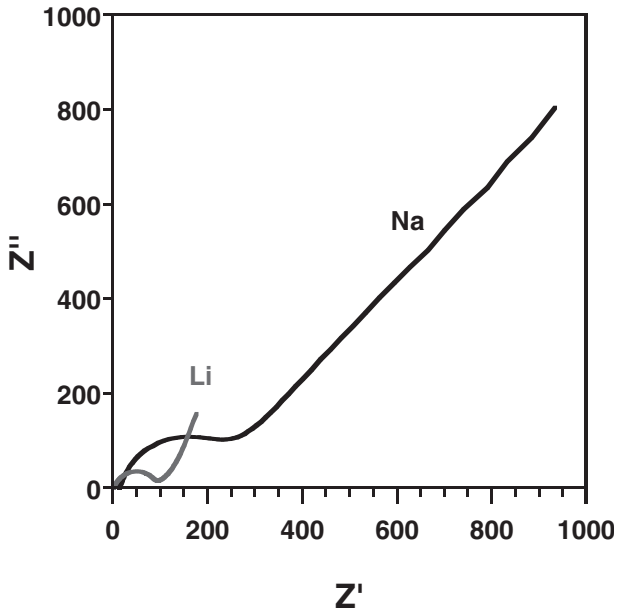

Figure 4. Nyquist plot of mesoporous C/Sn anodes in Na-ion and Li-ion cells after being charged to 2.0 V at 20 mA g^{-1} with a subsequent relaxation period of 2 h. The electrodes experienced five charge/discharge cycles before EIS measurements (Z′ and Z″ denote real and imaginary parts, respectively).

C/Sn composite at different current densities from 20 to 1000 mA g^{-1} in Na-ion and Li-ion batteries. The capacity of mesoporous C/Sn anodes decreases with increasing current in both Na-ion and Li-ion batteries, but capacity drop in Na-ion battery is faster than that in Li-ion batteries, which can be more clearly observed in the normalized rate capability in Figure 5b. At 400 mA g^{-1}, mesoporous C/Sn anodes in Li-ion batteries delivered 67% of the capacity at 20 mA g^{-1}, however, only 36% was provided by mesoporous C/Sn anodes in Na-ion batteries at the same current.

3. Conclusion

The electrochemical performance of mesoporous C/Sn composite anodes in Na-ion and Li-ion cells was systemically investigated and compared. Both sodium ions and lithium ions react with Sn to form stepwise alloys, but Na_xSn alloys are formed at lower potential (vs. Na) than Li_xSn alloys (vs. Li). The mesoporous C/Sn anodes in Na-ion batteries show similar cycling stablity but lower capacity and rate capability compared to mesoporous C/Sn anodes in Li-ion batteries. GITT analysis reveals that the electrochemical reaction of mesoporous C/Sn with Na has much larger resistance than does the reaction of C/Sn with Li, especially at the end of charge (ion extraction). Further EIS analysis of mesoporous C/Sn anodes at the end of charge shows that the high reaction resistance between C/Sn and Na is mainly attributed to the slow diffusion of Na ions in Sn and the high interfacial resistance of the Na–Sn reaction.

4. Experimental Section

Synthesis of Porous Carbon/Tin Nanoparticle Composite: The synthesis details can be found in the Supporting Information; here we briefly describe the synthesis. SnO_2 nanoparticles were dispersed into prepared polymer solution in dimethylformamide (DMF) by ultrasonication. After the mixture was dried under continuous stirring, the polymer/SnO_2 composite was carbonized with a heating ramp of 2 °C min^{-1} in flowing argon at 400 °C for 3 h and then 700 °C for an additional 3 h.

Material Characterization: Scanning electron microscopy (SEM) images were taken using a Hitachi SU-70 analytical ultra-high resolution SEM (Japan). X-ray diffraction (XRD) patterns were recorded by Bruker Smart1000 (Bruker AXS Inc., USA) using CuKα radiation. Thermogravimetric analysis (TGA) was carried out using a thermogravimetric analyzer (TA Instruments, USA) with a heating rate of 10 °C min^{-1} in air.

Electrochemical Measurements: The porous C/Sn composite was mixed with carbon black and carboxymethyl cellulose (CMC) binder to form slurry at the weight ratio of 70:15:15. The electrode was prepared by casting the slurry onto copper foil using a doctor blade and drying in a vacuum oven at 100 °C overnight. The thickness of the coating on Cu is approximately 20 μm and the Sn/C loading content is about 0.5 mg cm^{-2}.

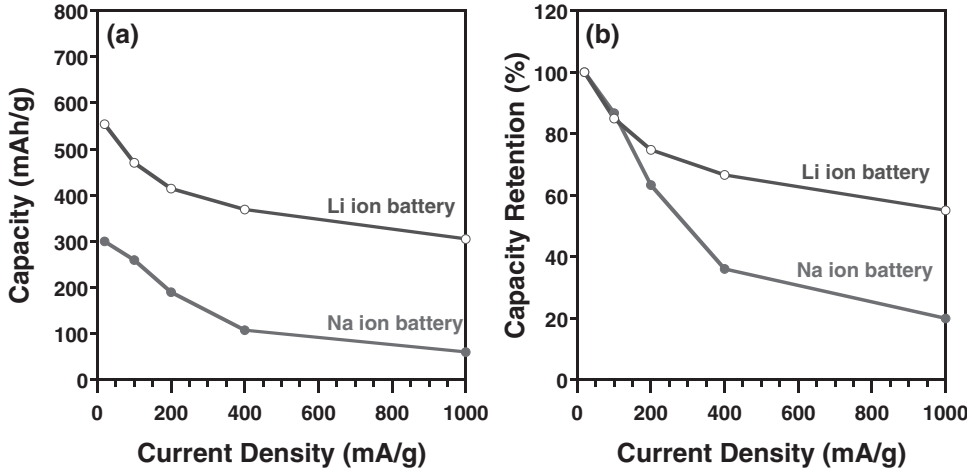

Figure 5. Comparison of rate capability at different currents between 0.02 and 1.5 V of Sn–Na and Sn–Li batteries: a) capacity retention, and b) capacity retention percentage at different current densities.

The electrode was cut into circular pieces with diameter 1.2 cm for coin-cell testing. Na-ion batteries were assembled with sodium as the counter electrode, 1 M $NaClO_4$ in a mixture of ethylene carbonate/dimethyl carbonate (EC/DMC, 1:1 by volume) as the electrolyte, and Celgard®3501 (Celgard, LLC Corp., USA) as the separator. Li-ion batteries were also fabricated at the same conditions using lithium as anode and 1 M $LiPF_6$ in a mixture of ethylene carbonate/diethyl carbonate (EC/DEC, 1:1 by volume) as the electrolyte. Electrochemical performance was tested using an Arbin battery test station (BT2000, Arbin Instruments, USA). Capacity was calculated on the basis of the total mass of the porous C/Sn composite. Cyclic voltammogramsat a scan rate of 0.05 mV s^{-1} between 0 and 2 V, GITT data, and EIS spectra of Sn/C anodes were recorded using a Solatron 1260/1287 Electrochemical Interface instrument (Solatron Metrology, UK). A Li foil for Li-ion batteries and an Na foil for Na-ion batteries were used as reference electrodes. GITT measurements were carried out by applying a pulse constant current (10 mA g^{-1} for Na-ion batteries and 20 mA g^{-1} for Li-ion batteries) with duration 30 min, followed by 4 h relaxation to reach an equilibrium voltage.

Supporting Information

Supporting Information is available from the Wiley Online Library or from the author.

Acknowledgements

The authors gratefully acknowledge the support of the Army Research Office under Contract No. W911NF1110231 (Dr. Robert Mantz, Program Manager), as well as an Ellen Williams Distinguished Postdoctoral Fellowship.

Received: May 14, 2012
Revised: June 22, 2012
Published online: September 3, 2012

[1] X. C. Lu, G. G. Xia, J. P. Lemmon, Z. G. Yang, *J. Power Sources* **2010**, *195*, 2431.
[2] L. Xiao, Y. Cao, J. Xiao, W. Wang, L. Kovarik, Z. Nie, J. Liu, *Chem. Commun.* **2012**, *48*, 3321.
[3] D. A. Stevens, J. R. Dahn, *J. Electrochem. Soc.* **2001**, *148*, A803.
[4] S. Wenzel, T. Hara, J. Janek, P. Adelhelm, *Energy Environ. Sci.* **2011**, *4*, 3342.
[5] P. Senguttuvan, G. Rousse, V. Seznec, J.-M. Tarascon, M. R. Palacín, *Chem. Mater.* **2011**, *23*, 4109.
[6] V. L. Chevrier, G. Ceder, *J. Electrochem. Soc.* **2011**, *158*, A1011.
[7] S. P. Ong, V. L. Chevrier, G. Hautier, A. Jain, C. Moore, S. Kim, X. Ma, G. Ceder, *Energy Environ. Sci.* **2011**, *4*, 3680.
[8] R. Alcántara, M. Jaraba, P. Lavela, J. L. Tirado, *Chem. Mater.* **2002**, *14*, 2847.
[9] P. Moreau, D. Guyomard, J. Gaubicher, F. Boucher, *Chem. Mater.* **2010**, *22*, 4126.
[10] K. T. Lee, T. N. Ramesh, F. Nan, G. Botton, L. F. Nazar, *Chem. Mater.* **2011**, *23*, 3593.
[11] J. F. Whitacre, A. Tevar, S. Sharma, *Electrochem. Commun.* **2010**, *12*, 463.
[12] S. Komaba, C. Takei, T. Nakayama, A. Ogata, N. Yabuuchi, *Electrochem. Commun.* **2010**, *12*, 355.
[13] Y. Kawabe, N. Yabuuchi, M. Kajiyama, N. Fukuhara, T. Inamasu, R. Okuyama, I. Nakai, S. Komaba, *Electrochem. Commun.* **2011**, *13*, 1225.
[14] C. Vidal-Abarca, P. Lavela, J. L. Tirado, A. V. Chadwick, M. Alfredsson, E. Kelder, *J. Power Sources* **2012**, *197*, 314.
[15] X. H. Ma, H. L. Chen, G. Ceder, *J. Electrochem. Soc.* **2011**, *158*, A1307.
[16] U. Kasavajjula, C. S. Wang, A. J. Appleby, *J. Power Sources* **2007**, *163*, 1003.
[17] C.-M. Park, J.-H. Kim, H. Kim, H.-J. Sohn, *Chem. Soc. Rev.* **2010**, *39*, 3115.
[18] C. Liu, F. Li, L.-P. Ma, H.-M. Cheng, *Adv. Mater.* **2010**, *22*, E28.
[19] J. C. Guo, X. L. Chen, C. S. Wang, *J. Mater. Chem.* **2010**, *20*, 5035.
[20] I. Kovalenko, B. Zdyrko, A. Magasinski, B. Hertzberg, Z. Milicev, R. Burtovyy, I. Luzinov, G. Yushin, *Science* **2011**, *334*, 75.
[21] M.-H. Park, M. G. Kim, J. Joo, K. Kim, J. Kim, S. Ahn, Y. Cui, J. Cho, *Nano Lett.* **2009**, *9*, 3844.
[22] Y. Yu, L. Gu, C. Wang, A. Dhanabalan, P. A. van Aken, J. Maier, *Angew. Chem. Int. Ed.* **2009**, *48*, 6485.
[23] Y. H. Xu, J. C. Guo, C. S. Wang, *J. Mater. Chem.* **2012**, *22*, 9562.
[24] Y. S. Jung, K. T. Lee, J. H. Ryu, D. Im, S. M. Oh, *J. Electrochem. Soc.* **2005**, *152*, A1452.
[25] X. W. Zhang, C. S. Wang, A. J. Appleby, F. E. Little, *Solid State Ionics* **2002**, *150*, 383.